Roles of nucleon resonances in Λ(1520) photoproduction off the proton

Jun He[1,2,*] and Xu-Rong Chen[1,2]

[1]*Institute of Modern Physics, Chinese Academy of Sciences, Lanzhou 730000, China*

[2]*Research Center for Hadron and CSR Physics, Institute of Modern Physics of CAS and Lanzhou University, Lanzhou 730000, China*

(Received 13 June 2012; revised manuscript received 14 August 2012; published 26 September 2012)

In this work the roles of the nucleon resonances in the Λ(1520) photoproduction off a proton target are investigated within the effective Lagrangian method. Besides the Born terms, including the contact term and s, u, and K exchanged t channels, the vector meson K^* exchanged t channel is considered in our investigation, which is negligible at low energy and important at high energy. The important nucleon resonances predicted by the constituent quark model (CQM) are considered and the results are found to be well comparable with the experimental data. Besides the dominant $D_{13}(2080)$, the resonance $[\frac{5}{2}^-]_2(2080)$ predicted by the CQM is found to be important for reproducing the experimental data. Other nucleon resonances are found to give small contributions in the channel considered in this work. With all important nucleon resonances predicted by the CQM, the prediction of the differential cross section at an energy up to 5.5 GeV is presented also; this can be checked by future CLAS experimental data.

DOI: 10.1103/PhysRevC.86.035204 PACS number(s): 14.20.Gk, 13.75.Cs, 13.60.Rj

I. INTRODUCTION

The study of nucleon resonance is an interesting area in hadron physics. As of now, the nucleon resonances around 2.1 GeV are still in confusion. The constituent quark model (CQM) predicted about two dozen nucleon resonances in this region, most of which are in the $n = 3$ shell. Only a few of them have been observed, with large uncertainties, as shown by the Particle Data Group (PDG) [1]. Among these nucleon resonances, $D_{13}(2080)$ attracts much attention due to its importance found in many channels, such as $\gamma p \to K^*\Lambda$ [2] and ϕ photoproduction [3]. In the analyses of the data for $\gamma p \to \eta' p$ by Zhang *et al.* and Nakayama and Haberzettl the contribution of $D_{13}(2080)$ is also found to be important for reproducing the experimental data [4,5]. However, in the recent work by Zhong and Zhao [6], the bumplike structure around $W = 2.1$ GeV is from the contribution of an $n = 3$ shell resonance $D_{15}(2080)$ instead of $D_{13}(2080)$. In Ref. [7], η photoproduction off the proton is studied in a chiral quark model, and a D_{15} resonance instead of a D_{13} state with mass about 2090 MeV is also suggested to reproduce the experimental data. Hence, more efforts should be made to figure out the nucleon resonances around 2.1 GeV.

After many years of efforts, the amount of experimental data for nucleon resonances below 2 GeV has accumulated while data above 2 GeV are still scarce. Due to the high threshold of Λ(1520) production, about 2 GeV, it is appropriate to enrich our knowledge of nucleon resonances, especially ones with mass larger than 2 GeV. There exist some old experiments for kaon photoproduciton off the nucleon with Λ(1520). In the late 1970s, researchers at the Stanford Linear Accelerator Center (SLAC) [8] used a 11-GeV photon beam on hydrogen to study the inclusive reaction $\gamma p \to K^+ Y$, where Y represents a produced hyperon. The LAMP2 Collaboration at Daresbury [9] studied the exclusive reaction $\gamma p \to K^+\Lambda^*$ with $\Lambda^* \to pK^-$ at photon energies ranging from 2.8 to 4.8 GeV. In recent years, excited by the claimed finding of the pentaquark Θ with a mass of about 1.540 GeV reported by the LEPS Collaboration in 2003 [10], many experiments have been performed in the Λ(1520) energy region due to the close mass of Λ(1520) and Θ. Though the existence of the pentaquark is doubtful based on later more precise experiments, many experimental data on Λ(1520) photoproduction have been accumulated, which provides an opportunity to understand the reaction mechanism of Λ(1520) photoproduction off the nucleon and the possible nucleon resonances in this reaction.

The LEPS experiment (labeled as LEPS09 in this work) at Spring-8 measured Λ(1520) photoproduction with liquid hydrogen and deuterium targets at photon energies below 2.4 GeV [11]. A large asymmetry of the production cross sections in the proton and neutron channels was observed at backward $K^{+/0}$ angles. This supports the conclusion by Nam and Kao [12] that the contact term, with t-channel K exchange under gauge invariance, plays the most important role in Λ(1520) photoproduciton and the contribution from resonances $D_{13}(2080)$ is small and negligible. Differential cross sections and photon-beam asymmetries for the $\gamma p \to K^+\Lambda(1520)$ reaction have been measured by the LEPS Collaboration (labeled as LEPS10) with linearly polarized photon beams at energies from the threshold to 2.4 GeV at $0.6 < \cos\theta^K_{\rm CM} < 1$ [13]. A new bump structure was found at $W \simeq 2.1$ GeV in the cross sections. Xie and Nieves suggested that the bump structure could be reproduced by including the resonance $D_{13}(2080)$ [14]. For the polarized symmetry, the theoretical result by Xie and Nieves seems to have an inverse sign compared with the LEPS10 data. The model by Nam *et al.* also gives near zero polarized asymmetry [13].

In Refs. [15,16], the electromagnetic and strong decays were studied in the CQM, from which the contributions of the nucleon resonances in phtoproductions can be calculated in Ref. [17]. In this work we will investigate Λ(1520) photoproduction within the effective Lagrangian method, with the nucleon resonances included according to the CQM

*junhe@impcas.ac.cn

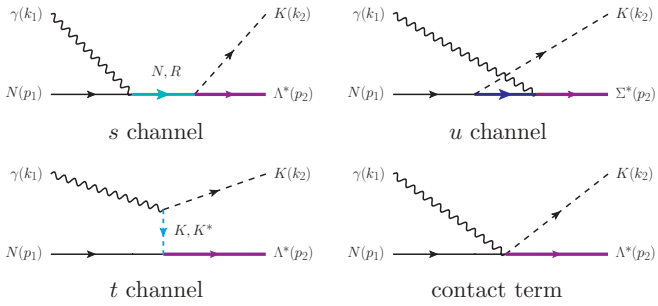

FIG. 1. (Color online) The diagrams for the s, u, and t channels and contact term.

prediction, to find the roles the nucleon resonances, especially the D_{13} and D_{15} states around 2.1 GeV, played in the reaction mechanism.

This paper is organized as follows. After the introduction, we will present the effective Lagrangian used in this work and the amplitudes based on the effective Lagrangian. The differential cross section at low energy and the prediction at high energy will be given in Sec. III. Finally, the paper ends with a brief summery.

II. FORMALISM

The mechanisms for $\Lambda(1520)$ photoproduction off a nucleon with K is shown in the diagrams in Fig. 1. In this work, due to the small contribution from the u channel as shown in the literature [12,14,18] it is not considered. Besides the Born terms, including the s channel, the K exchanged t channel, and the contact term, the contributions from the K^* exchanged t and resonance (R) intermediate s channels are considered in the current work.

A. Born terms

The Lagrangians used in the Born terms are [12,14]

$$\begin{aligned}
\mathcal{L}_{\gamma KK} &= ieQ_K[(\partial^\mu K^\dagger)K - (\partial^\mu K)K^\dagger]A_\mu,\\
\mathcal{L}_{\gamma NN} &= -e\bar{N}\left[Q_N \not{A} - \frac{\kappa_N}{4M_N}\sigma^{\mu\nu}F^{\mu\nu}\right]N,\\
\mathcal{L}_{KN\Lambda^*} &= \frac{g_{KN\Lambda^*}}{M_{\Lambda^*}}\bar{\Lambda}^{*\mu}\partial_\mu K\gamma_5 N + \text{H.c.},\\
\mathcal{L}_{\gamma KN\Lambda^*} &= -\frac{ieQ_N g_{KN\Lambda^*}}{M_{\Lambda^*}}\bar{\Lambda}^{*\mu}A_\mu K\gamma_5 N + \text{H.c.},
\end{aligned} \tag{1}$$

where $F^{\mu\nu} = \partial^\mu A\nu - \partial^\nu A_\mu$ with A^μ, N, K, and Λ^* as the photon, nucleon, kaon, and $\Lambda^*(1520)$ fields. Here Q_h is the charge in the units of $e = \sqrt{4\pi\alpha}$. The anomalous magnetic momentum $\kappa = 1.79$ for the proton. The coupling constant $g_{KN\Lambda^*} = 10.5$ obtained form the decay width of $\Lambda^* \to NK$ from the PDG [1].

For the K^* exchange t channel, we need the following Lagrangians:

$$\mathcal{L}_{\gamma KK^*} = g_{\gamma KK^*}\epsilon_{\mu\nu\sigma\rho}(\partial^\mu A^\nu)(\partial^\sigma K^{*\rho})K + \text{H.c.}, \tag{2}$$

$$\mathcal{L}_{K^*N\Lambda^*} = -\frac{ig_{K^*N\Lambda^*}}{m_V}\bar{\Lambda}^{*\mu}\gamma^\nu F_{\mu\nu}N + \text{H.c.}, \tag{3}$$

with the coupling constant $g_{\gamma K^\pm K^{*\mp}} = 0.254\ \text{GeV}^{-1}$ extracted from the decay width from the PDG [1]. A Reggeized treatment will be applied to the t channel. As discussed in Ref. [19], the coupling constant for the Reggeized treatment can be different from the one in the effective Lagrangian approach. Here we do not adopt the value of about 1 determined from the SU(6) model [20], but we use the larger one, about 10, from the quark model [20] and phenomenological fitting of Nam *et al.* [18] and Totiv *et al.* [21].

The scattering amplitude for photoproduction can be written as follows:

$$-i\mathcal{T}_{\lambda_{\Lambda^*},\lambda_\gamma\lambda_N} = \bar{u}_\mu(p_2,\lambda_{\Lambda^*})A^{\mu\nu}u(p_1,\lambda_N)\epsilon_\nu(k_1,\lambda_\gamma), \tag{4}$$

where ϵ, u_1, and u_2^μ denote the photon polarization vector, nucleon spinor, and Rarita-Schwinger vector-spinor, respectively. λ_{Λ^*}, λ_γ, and λ_N are the helicities for the $\Lambda(1520)$, the photon, and the nucleon, respectively.

The amplitudes for Born s and t channels and the contact term are

$$\begin{aligned}
A_s^{\mu\nu} &= -\frac{eg_{KN\Lambda^*}}{m_K}\frac{1}{s-M_N^2}k_2^\mu\gamma_5\\
&\quad\times\left[Q_N((\not{p}_1+M_N)F_c + \not{k}_1F_s)\gamma^\nu\right.\\
&\quad\left.+\frac{\kappa_N}{2M_N}(\not{k}_1+\not{p}_1+M_N)\gamma^\nu\not{k}_1F_s\right],
\end{aligned} \tag{5}$$

$$A_t^{\mu\nu} = \frac{eQ_Kg_{KN\Lambda^*}F_c}{m_K}\frac{1}{t-m_K^2}q^\mu k_2^\nu\gamma_5, \tag{6}$$

$$A_{\text{cont.}}^{\mu\nu} = \frac{eQ_Ng_{KN\Lambda^*}F_c}{m_K}g^{\mu\nu}\gamma_5, \tag{7}$$

where s, t, and u indicate the Mandelstam variables.

The amplitude for K^* exchange is

$$\begin{aligned}
A_t^{K^*} &= \frac{ig_{\gamma KK^*}g_{K^*NB}F_V}{m_{K^*}}\frac{1}{t-m_{K^*}^2}\left(\epsilon_{\sigma\rho\xi\nu}k_1^\rho k_2^\xi\right)\\
&\quad\times\gamma_\nu\left[\left(k_1^\mu-k_2^\mu\right)g^{\nu\sigma}+\left(k_1^\nu-k_2^\nu\right)g^{\mu\sigma}\right].
\end{aligned} \tag{8}$$

The form factors are introduced in the same form:

$$F_i = \left(\frac{n\Lambda_i^4}{n\Lambda_i^4+(q_i^2-M_i^2)^2}\right)^n, \tag{9}$$

$$F_c = F_s + F_t - F_sF_t \tag{10}$$

where i means s, t, V, and R, corresponding to s channel, t channel, vector exchange t channel, and resonance intermediate s channel.

To describe the behavior at high photon energy, we introduce the pseudoscalar and vector strange-meson Regge trajectories as follows [21–23]:

$$\begin{aligned}
\frac{1}{t-m_K^2} &\to \mathcal{D}_K = \left(\frac{s}{s_0}\right)^{\alpha_K}\frac{\pi\alpha'_K}{\Gamma(1+\alpha_K)\sin(\pi\alpha_K)},\\
\frac{1}{t-m_{K^*}^2} &\to \mathcal{D}_{K^*} = \left(\frac{s}{s_0}\right)^{\alpha_{K^*}-1}\frac{\pi\alpha'_{K^*}}{\Gamma(\alpha_{K^*})\sin(\pi\alpha_{K^*})},
\end{aligned} \tag{11}$$

where α'_{K,K^*} indicates the slope of the trajectory. α_{K,K^*} is the linear trajectory of the meson for even or odd spin, which is a

TABLE I. Parameters for the Reggeized treatment in units of GeV^2.

$s_{Reg} = 3$	$t_{Reg} = 0.1$	$s_0 = 1$	$t_0 = 0.08$

function of t assigned as follows:

$$\alpha_K = 0.70\ \text{GeV}^{-2}\left(t - m_K^2\right), \tag{12}$$

$$\alpha_{K^*} = 1 + 0.85\ \text{GeV}^{-2}\left(t - m_{K^*}^2\right). \tag{13}$$

To restore the gauge invariance, we redefine the relevant amplitudes as follows [12]:

$$\begin{aligned} &i\mathcal{M}_K + i\mathcal{M}_s^E + i\mathcal{M}_c \\ &\quad\to i\mathcal{M}_K^{\text{Regge}} + \left(i\mathcal{M}_s^E + i\mathcal{M}_c\right)\left(t - M_K^2\right)\mathcal{D}_K. \end{aligned} \tag{14}$$

The Reggeized treatment should work completely at high photon energies and interpolate smoothly to low photon energy. It has been considered by Toki *et al.* [19] and Nam and Kao [12] by introducing a weighting function. Here we adopt the treatment by Namand Kao and set

$$F_{c,v} \to \bar{F}_{c,v} \equiv \left[\left(t - m_{K,K^*}^2\right)\mathcal{D}_{K,K^*}\right]\mathcal{R} + F_{c,v}(1 - \mathcal{R}), \tag{15}$$

where $\mathcal{R} = \mathcal{R}_s\mathcal{R}_t$ with

$$\begin{aligned} \mathcal{R}_s &= \frac{1}{2}\left[1 + \tanh\left(\frac{s - s_{\text{Regge}}}{s_0}\right)\right], \\ \mathcal{R}_t &= 1 - \frac{1}{2}\left[1 + \tanh\left(\frac{|t| - t_{\text{Regge}}}{t_0}\right)\right]. \end{aligned} \tag{16}$$

In this work the values of the four parameters for the Reggeized treatment are chosen as in Nam and Kao, as presented in Table I.

B. Nucleon resonances

In Ref. [14], the $D_{13}(2080)$ is considered to reproduce the bump structure near 2.1 GeV. In this work all resonances predicted by the CQM will be considered. The Lagrangians for the resonances with arbitrary half-integer spin are [24–26]

$$\mathcal{L}_{\gamma NR(\frac{1}{2}^{\pm})} = \frac{ef_2}{2M_N}\bar{N}\Gamma^{(\mp)}\sigma_{\mu\nu}F^{\mu\nu}R + \text{H.c.}, \tag{17}$$

$$\begin{aligned} \mathcal{L}_{\gamma NR(J^{\pm})} &= \frac{-i^n f_1}{(2m_N)^n}\bar{B}^*\gamma_\nu\partial_{\mu_2}\cdots\partial_{\mu_n}F_{\mu_1\nu}\Gamma^{\pm(-1)^{n+1}}R^{\mu_1\mu_2\ldots\mu_n} \\ &\quad + \frac{i^{n+1}f_2}{(2m_N)^{n+1}}\partial_\nu\bar{B}^*\partial_{\mu_2}\cdots\partial_{\mu_n}F_{\mu_1\nu}\Gamma^{\pm(-1)^{n+1}} \\ &\quad \times R^{\mu_1\mu_2\ldots\mu_n} + \text{H.c.}, \end{aligned} \tag{18}$$

where $R_{\mu_1\cdots\mu_n}$ is the field for the resonance with spin $J = n + 1/2$, and

$$\Gamma^{(\pm)} = (i\gamma_5, 1) \tag{19}$$

for the different resonance parit. The Lagrangians are also adopted from the previous works on nucleon resonances with spins 3/2 or 5/2 [12,14,17,27].

The Lagrangian for the strong decay can be written as

$$\mathcal{L}_{RK\Lambda^*} = \frac{ig_2}{2m_K}\partial_\mu K\bar{\Lambda}_\mu^*\Gamma^{(\pm)}R, + \text{H.c.}, \tag{20}$$

$$\begin{aligned} \mathcal{L}_{RK\Lambda^*} &= \frac{i^{2-n}g_1}{m_P^n}\bar{B}_{\mu_1}^*\gamma_\nu\partial_\nu\partial_{\mu_2}\cdots\partial_{\mu_n}P\Gamma^{\pm(-1)^n}R^{\mu_1\mu_2\ldots\mu_n} \\ &\quad + \frac{i^{1-n}g_2}{m_P^{n+1}}\bar{B}_\alpha^*\partial_\alpha\partial_{\mu_1}\partial_{\mu_2}\cdots\partial_{\mu_n}P\Gamma^{\pm(-1)^n}R^{\beta\mu_1\mu_2\ldots\mu_n} \\ &\quad + \text{H.c.} \end{aligned} \tag{21}$$

The corresponding propagator for the arbitrary half-integer spin can be found in Appendix A.

In this work the coupling constants f_1, f_2, g_1, and g_2 will be determined by the radiative and strong decays of the nucleon resonances. For a $j = \frac{1}{2}$ resonance, the magnitudes of the coupling constants f_1 and h_1 can be determined by the radiative and strong decay widths. However, for nucleon resonances with high spin ($j \geqslant \frac{3}{2}$), the decay widths are not enough to determine coupling constants f_1 and f_2 for radiative decay or h_1 and h_2 for strong decay [17]. Therefore, we need to know the decay amplitudes to determine the coupling constants uniquely.

For radiative decay, the helicity amplitudes are important physical quantities and can be extracted from the experimental photoproduction data. The definition of the helicity amplitude is

$$A_\lambda = \frac{1}{\sqrt{2|\boldsymbol{k}|}}\langle\gamma(\boldsymbol{k}, 1)N(-\boldsymbol{k}, \lambda - 1)| - iH_\gamma|R(\boldsymbol{0}, \lambda)\rangle, \tag{22}$$

where $|\boldsymbol{k}| = (M_R^2 - M_N^2)/(2M_R)$, $\boldsymbol{k}$ is the momentum of the photon in the center-of-mass system of the decaying nucleon resonance R, and $\lambda = 1/2$ or $3/2$ is the helicity. Since there are two amplitudes $A_{1/2}$ and $A_{3/2}$ for the resonances with $J > 1/2$, the coupling constants f_1 and f_2 in $\mathcal{L}_{RN\gamma}$ can be extracted from the helicity amplitudes of the resonance R.

The coupling constants g_1 and g_2 can be calculated analogously by the following relation for the decay amplitude:

$$\begin{aligned} &\langle K(\boldsymbol{q})\,\Lambda^*(-\boldsymbol{q}, m_f)| - i\,\mathcal{H}_{\text{int}}|R(\boldsymbol{0}, m_J)\rangle \\ &\quad = 4\pi M_R\sqrt{\frac{2}{q}}\sum_{\ell, m_\ell}\left\langle \ell\, m_\ell\, \frac{3}{2}\, m_f \middle| J\, m_J\right\rangle Y_{\ell m_\ell}(\hat{\boldsymbol{q}})G(\ell), \end{aligned} \tag{23}$$

where $\langle \ell\, m_\ell\, \frac{3}{2}\, m_f | J\, m_J\rangle$, $Y_{\ell m_\ell}(\hat{\boldsymbol{q}})$, and $G(\ell)$ are the Clebsch-Gordan coefficient, the spherical harmonics function, and the partial wave decay amplitude, respectively. The explicit derivation is presented in Appendix B.

III. RESULTS

With the Lagrangians presented in the previous section, Λ(1520) photoproduction can be studied. With the contributions from nucleon resonances determined by the decay amplitudes, we will determine the parameters used in our model first. Then the observables, such as differential cross section, will be calculated and compared with experiment.

A. Contributions from nucleon resonances

The different cross section have been measured in LEPS09 and LEPS10 experiments. As found by Nam and Kao [12] and Xie and Nieves [14], the most important contribution at low

TABLE II. The nucleon resonances considered. The mass m_R, helicity amplitudes A_λ, and partial wave decay amplitudes $G(\ell)$ are in units of MeV, $10^{-3}/\sqrt{\text{GeV}}$, and $\sqrt{\text{MeV}}$, respectively. The last column is for χ^2 after turning off the corresponding nucleon resonance with $\chi^2 = 1.38$ in the full model.

State	PDG	M_R	$A^p_{1/2}$	$A^p_{3/2}$	$G(\ell_1)$	$G(\ell_2)$	$\sqrt{\Gamma_{\Lambda(1520)K}}$	χ^2
$[N\frac{1}{2}^-]_3(1945)$	$N(2090)S_{11}{}^*$	2090	12		$6.4^{+5.7}_{-6.4}$		$6.4^{+5.7}_{-6.4}$	1.89
$[N\frac{3}{2}^-]_3(1960)$	$N(2080)D_{13}{}^{**}$	2150	36	−43	$-2.6^{+2.6}_{-2.8}$	$-0.2^{+0.2}_{-1.3}$	$2.6^{+2.9}_{-2.6}$	12.42
$[N\frac{5}{2}^-]_2(2080)$		2080	−3	−14	$-4.7^{+4.7}_{-1.2}$	$-0.3^{+0.3}_{-0.8}$	$4.7^{+1.3}_{-4.7}$	4.01
$[N\frac{5}{2}^-]_3(2095)$	$N(2200)D_{15}{}^{**}$	2200	−2	−6	$-2.4^{+2.4}_{-2.0}$	$-0.1^{+0.1}_{-0.3}$	$2.4^{+2.0}_{-2.4}$	1.59
$[N\frac{7}{2}^-]_1(2090)$	$N(2190)G_{17}{}^{****}$	2190	−34	28	$-0.5^{+0.4}_{-0.6}$	$0.0^{+0.0}_{-0.0}$	$0.5^{+0.6}_{-0.4}$	1.48
$[N\frac{7}{2}^+]_2(2390)$		2390	−14	−11	$3.1^{+0.8}_{-1.2}$	$0.3^{+0.3}_{-0.2}$	$3.1^{+0.8}_{-1.2}$	1.79

energy for the differential cross section is from the contact term. The bump structure is from $D_{13}(2080)$, as suggested by Xie and Nieves by fitting the LEPS10 data. In this work we will use the helicity amplitudes A_λ and the partial wave decay amplitudes $G(\ell)$ to describe the decays of the resonances. In the experiment, the helicity amplitudes for the nucleon resonances with smaller mass are determined well while the ones for the resonances with larger mass, especially the resonances with mass larger than 2 GeV, which are considered in this work, are still not well determined and cannot be compared well with the theoretical predictions.

In this work we will adopt the values obtained in the typical CQM by Capstcik and Reborts [15,16] as input. In their works the partial wave decay amplitudes are also provided. The nucleon resonances considered in the calculation are listed in Table II. The threshold of $\gamma p \to K\Lambda(1520)$ is about 2.01 GeV, so only the nucleon resonances above 2.01 GeV are included in the calculation. In the works by Capstcik [15,16], about two dozen nucleon resonances with spins up to 15/2 are calculated. In the current work, to simplify the calculation only nucleon resonances with large radiative decay and strong decay to $\Lambda(1520)K$ are used in the calculation of $\Lambda(1520)$ photoproduction, which is reasonable in physics also.

For the masses of the nucleon resonances, the suggested values provided by the PDG [1] are preferred and, for the resonances not listed in the PDG, the prediction from the CQM will be adopted. Due to the dominance of $D_{13}(2080)$ in the current channel, we adopt the mass suggested by Xie and Nieves [14], 2150 MeV, which is a little larger than the suggested value by the PDG, 2080 MeV. In order to prevent the proliferation of free parameters, the decay widths for all nucleon resonances are set to 200 MeV. For the cutoffs for the nucleon resonances, the typical value $\Lambda_R = 1$ GeV with $n = 1$ is used. Therefore, the contributions from the nucleon resonances are fixed because the helicity amplitudes and partial wave decay amplitudes predicted by the CQM are adopted in the calculation to determine the coupling constants.

B. Determination of model parameters

The contributions from the Born terms are very important, as shown in previous works. The magnitudes of contributions from the contact term and u, s, and K exchange t channels only depend on the coupling constant $g_{KN\Lambda^*}$, which is determined by the experimental decay width of $\Lambda^* \to NK$, and the cut off Λ. To reproduce the LEPS10 data, a cutoff of $\Lambda = 0.6$ GeV and $n = 1$ should be used. With this setting, the s-channel contribution is found to be very small.

Now we turn to the contribution of the vector meson K^* exchange. We consider the differential cross section at 11 GeV from SLAC measurements, where the contributions from the contact term and the t channel should be dominant, which is confirmed by the results shown in Fig. 2.

One can find that, at 11 GeV, the contribution from the contact terms is still most important while the contribution from the K exchanged t channel becomes more important compared with that at low energy. However, it is still not enough to reproduce the experimental data by including only the contributions from the contact term and K exchanged t channel. In the work by Nam and Nieves [12] the differential cross section can be reproduced by adopting a larger cutoff of $\Lambda = 0.675$ GeV. However, with such a value of Λ, the differential cross section at low energy cannot be well reproduced. The parameters for the Reggeized treatment, $s_{0,Reg}$ and $t_{0,Reg}$ in Table I, are varied and it is found to be impossible to compensate for the deficiency. Here we include the contribution of the vector meson K^* exchange. With cutoff $\Lambda_V = 0.8$ GeV and $n = 2$, the differential cross section from the SLAC experiment is well reproduced, as shown in Fig. 2. In the figure one can find that the contribution from vector meson

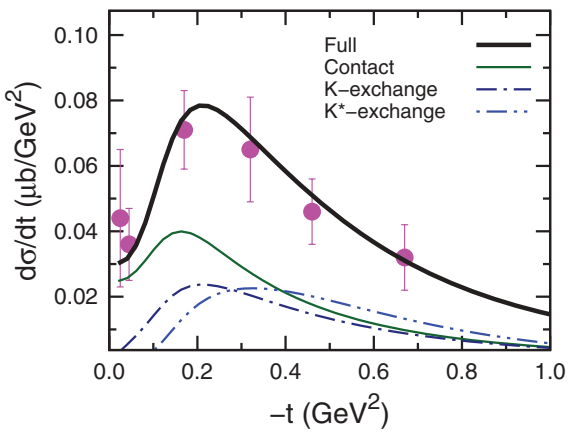

FIG. 2. (Color online) The differential cross section $d\sigma/dt$ at 11 GeV and compared with the data from SLAC [8]. The thick full line is for the result in the full model. The full, dash-dotted, and dash-dot-dotted lines are for the contact term, K exchange channel, and K^* exchange channel, respectively.

TABLE III. The coupling constants for the K and K^* exchanged channels and cutoffs in units of GeV.

$g_{\gamma K^\pm K^{*\mp}}$	0.254	$g_{KN\Lambda^*}$	10.5	$\bar{g}_{K^*N\Lambda^*}$	10
Λ	0.6	Λ_V	0.8	Λ_R	1

K^* exchange is comparable with the one from pseudoscalar meson K exchange.

The determined cutoffs and coupling constants for the Born terms and the K^* exchange are collected in Table III.

C. Differential cross section

With the parameters determined and the amplitudes presented in Table II, the theoretical results for the differential cross section at low energy are presented in Fig. 3 and compared with the LEPS10 experiment. As shown in the figure, the experimental data are well reproduced in our model. The dominant contributions are from the Born terms where the contact term plays the most important role. At low energy the K exchange contribution is smaller but visible while the vector meson K^* exchanged contribution is negligible.

To find the importance of each nucleon resonance, the χ^2 value for the differential cross section from threshold to 2.5 GeV from the LEPS10 experiment and those at 11 GeV from SLAC are calculated. The χ^2 value obtained in the current work is 1.38, which is a little larger than the 1.2 obtained by Xie and Nieves but close to 1.4 in their fitting with strong coupling constants as free parameters [14]. We remind the reader that in the current work both electromagnetic and strong coupling constants are determined from the CQM predictions with the physics choice of the mass and cutoff for the nucleon resonance.

To check the role of the nucleon resonance played in Λ(1520) photoproduction, we list the χ^2 value after turning off the corresponding nucleon resonance in Table II. Compared with the value $\chi^2 = 1.38$ in the full model, χ^2 after turning off the $D_{13}(2080)$ resonance increases significantly to 12.42, which confirms the dominant role played by this resonance, as suggested by Xie and Nieves [14]. Besides the dominant $D_{13}(2080)$, the contribution from a D_{15} resonance is also important. After turning off $[\frac{5}{2}^-]_2(2080)$, the χ^2 will increase to 4.01 due to the interference effect mainly. Simultaneously the $[\frac{5}{2}^-]_3(2095)$ is found to be unimportant with $\chi^2 = 1.59$ after being turned off. In the PDG paper [1] a D_{15} state $N(2200)$ is listed, which is assigned to the $[\frac{5}{2}^-]_3(2095)$ state in the CQM usually [15]. The predicted decay amplitudes in $N\pi$ and ΛK channels for $[\frac{5}{2}^-]_3(2095)$ are close to those for $[\frac{5}{2}^-]_2(2080)$ [15]. To check whether the D_{15} state $[\frac{5}{2}^-]_2(2080)$ instead of $[\frac{5}{2}^-]_3(2095)$ is the observed resonance $N(2200)$ listed by the

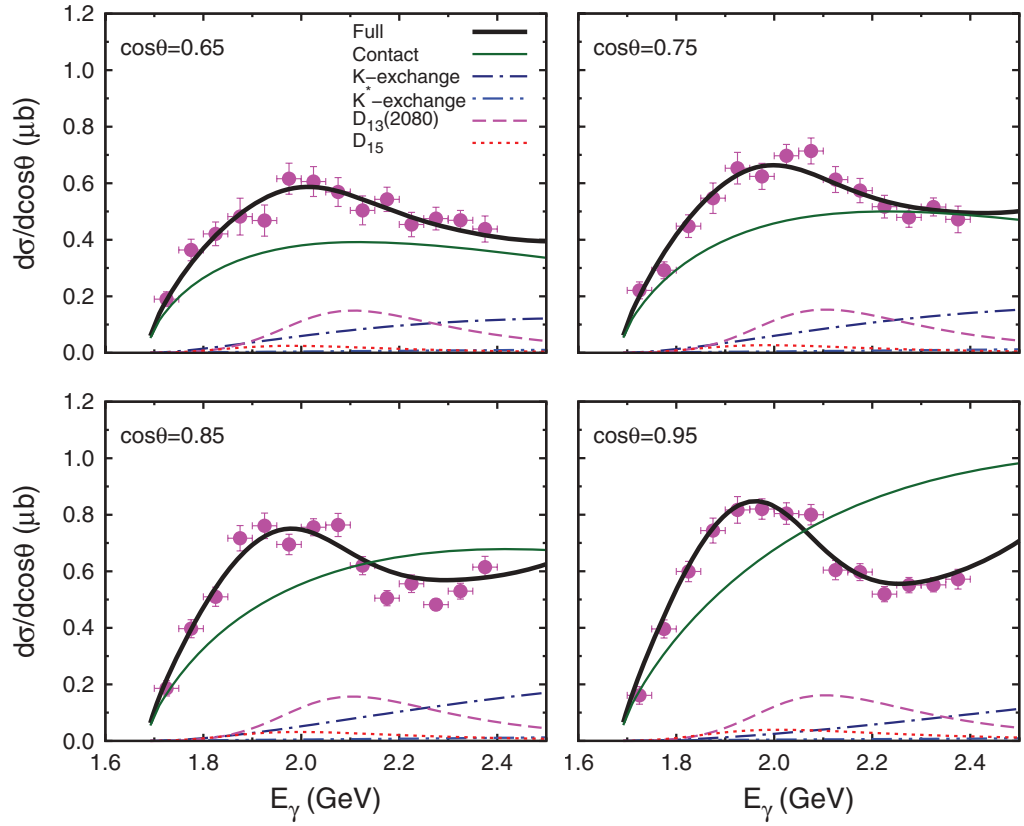

FIG. 3. (Color online) The differential cross section $d\sigma/d\cos\theta$ at low photon energy and compared with the data from LEPS10. The thick full line is for the results in the full model.The full, dash-dotted, and dash-dot-dotted lines are for the contact term, the K exchange channel, and the K^* exchange channel, respectively. The dashed (dotted) line is for nucleon resonance $D_{13}(2080)$ (D_{15}).

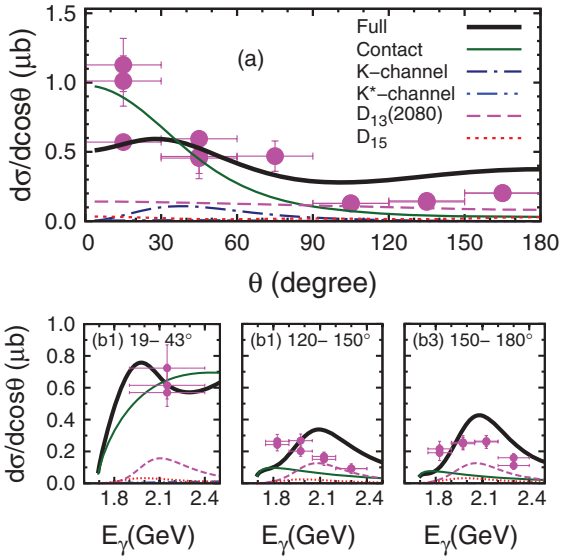

FIG. 4. (Color online) (a) The differential cross section $d\sigma/d\cos\theta$ with the variation of θ at a photon energy of 2.2 GeV compared with the data from LEPS09 at a photon energy of 1.9–2.4 GeV. (b1)–(b3) The differential cross section $d\sigma/d\cos\theta$ with the variation of photon energy E_γ. The notation is as in Fig. 3.

PDG, we vary the mass of $[\frac{5}{2}^-]_2(2080)$ to 2.2 GeV and a χ^2 of about 4 is found. This indicates that the experimental data require that the mass of $[\frac{5}{2}^-]_2(2080)$ should be about 2.08 GeV. Hence $[\frac{5}{2}^-]_2(2080)$ should not be assigned to $N(2200)$ due to the large mass discrepancy of about 100 MeV.

To give a picture around the resonance poles, we calculate $d\sigma/d\cos\theta$ against θ at 2.2 GeV and compare with LEPS09 data as shown in Fig. 4.

The experimental data are reproduced generally in our model. One can find that the general shape for the differential cross section against θ is mainly formed by the contact term contribution. The slow increase in the backward direction is from the resonance contributions. For differential cross sections with variation of E_γ, the nucleon resonances give contributions larger than that from the contact term and are responsible for the bump at backward angles.

D. Polarized asymmetry

The polarized asymmetry was measured in the LEPS10 experiment. Nearly zero polarized asymmetry was obtained in the model by Nam *et al.* [13]. In Ref. [14] the result suggested that the sign should be reversed compared with the experiment. In this work, a result similar to that of Ref. [14] is obtained, as shown in Fig. 5. It suggests that further improvement may be needed based on the effective Lagrangian method, such as including unitary, coupled-channel effects.

E. Prediction of differential cross section at high energy

In the above sections, all parameters, such as cutoffs, are determined and the contributions from nucleon resonances are introduced by the CQM predictions. With these parameters the differential cross sections at energy below 2.5 GeV and

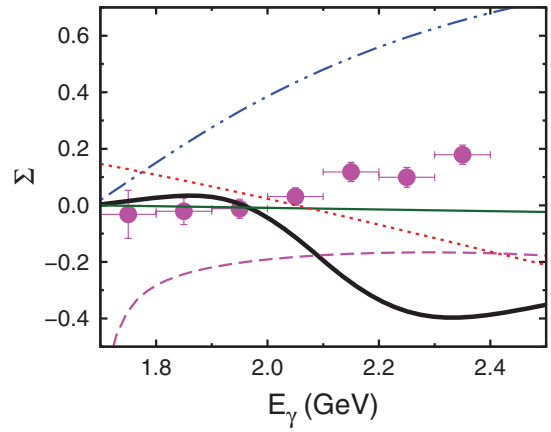

FIG. 5. (Color online) Polarization asymmetry compared with LEPS10. The notation is as in Fig. 3.

at 11 GeV have been reproduced well. Hence it is possible to give a prediction for energy higher than 2.5 GeV. Recently, the CLAS Collaboration reported $\Lambda(1520)$ photoproduction measured at photon energy from 1.87 to 5.5 GeV and some preliminary results have been obtained in the $eg3$ run [28]. The g_{11} experiment also ran in this energy region. Therefore, it is meaningful to make some predictions. The differential cross sections $d\sigma/d\theta$ predicted by the model obtained in this work are presented in Fig. 6.

The contributions from $D_{13}(2080)$ and $D_{15}(2080)$ are still the most important as well as at low energy. The $[\frac{7}{2}^-]_2(2390)$ is small at high energy though it has higher mass. The contribution from the contact term plays the most important role for energy up to 5.5 GeV, especially at forward angles, while the contributions from the two resonances will decrease rapidly at photon energy larger than the energy point corresponding to the Breit-Wigner mass.

The dominance of contact contribution at the higher photon energy can be observed more obviously in the differential cross section $d\sigma/dt$, as shown in Fig. 7.

At high photon energy, the contact contribution is several times larger than the vector meson K^* exchange and the contributions from the resonances are negligible. The contributions from the nucleon resonances $D_{13}(2080)$ and D_{15} are important

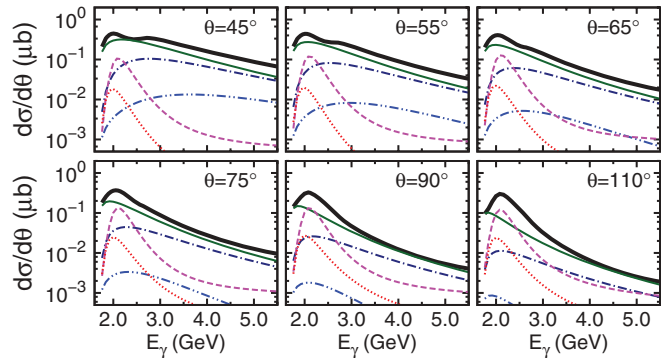

FIG. 6. (Color online) The differential cross section $d\sigma/d\theta$ with the variation of photon energy E_γ predicted in this work. The notation is as in Fig. 3.

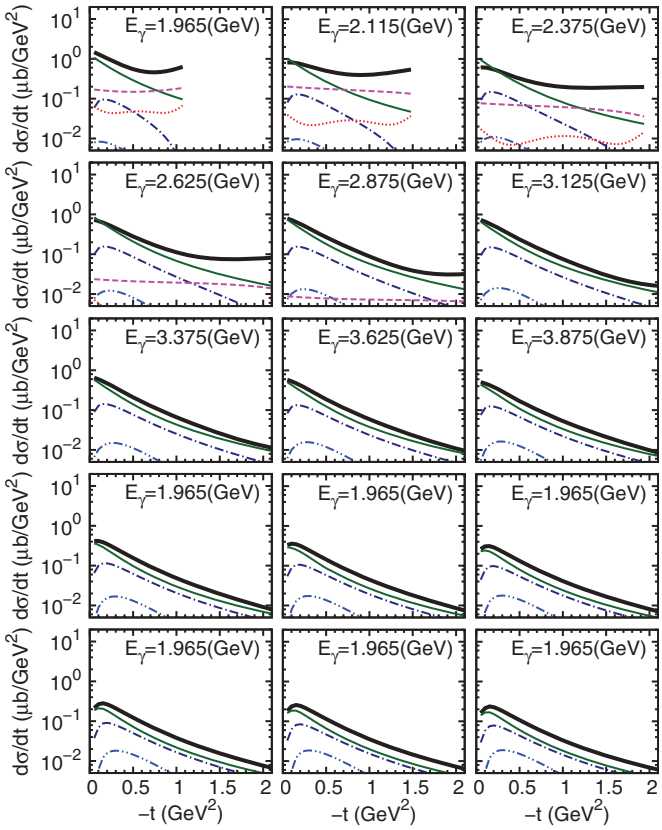

FIG. 7. (Color online) The differential cross section $d\sigma/dt$ with variation of $-t$ predicted in this work. The notation is as in Fig. 3.

at low energy and exhibit a slow increase in the large-$|t|$ region.

F. Total cross section

As of now, there only exist a few experimental data for the total cross section. The data from the SAPHIR experiment are only at low energy [29] while the LAMP2 experiment gives some data at high energy [9]. In Fig. 8, we show the theoretical results in our model and compared with the experimental data.

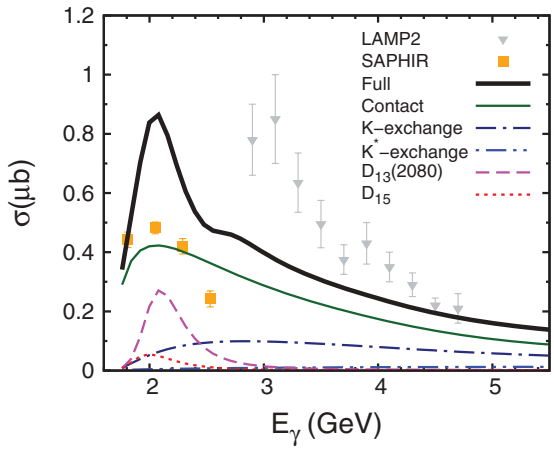

FIG. 8. (Color online) Total cross section σ with the variation of the photon energy E_γ. The notation for the theoretical results is as in Fig. 3. The data are from Refs. [9,29].

As shown in Fig. 8, though the two sets of data do not overlap in energy, it can be easily found that they are not consistent with each other. The old LAMP2 data are higher than the SAPHIR data systemically. Our result is just in the middle of the two sets of data. As indicted in the differential cross section, the nucleon resonances $D_{13}(2080)$ and D_{15} are responsible for the peak around 2.1 GeV.

IV. SUMMERY

In this work we investigated Λ(1520) photoproduction in the $\gamma N \to K\Lambda(1520)$ reaction within the effective Lagrangian method. The contact term is dominant in the interaction mechanism and K exchanged t channel is important except at energy near the threshold. The K^* exchange t channel plays an important role in the high-energy region at 11 GeV but is negligible at low energy.

The contributions of nucleon resonances are determined by the radiative and strong decay amplitudes predicted by the constituent quark model. The results shows that $D_{13}(2080)$ is the most important nucleon resonance in Λ(1520) photoproduction and is responsible for the bump structure in the LEPS10 experiment. A nucleon resonance $[\frac{5}{2}^-]_2(2080)$ predicted by the CQM with mass of about 2100 MeV, which cannot be assigned as $N(2200)$, is also essential for reproducing the experimental data around 2.1 GeV. The contributions from other nucleon resonances are small and even negligible.

With the contributions from the Born terms and nucleon resonances, the experimental data for differential cross sections can be reproduced while there exists large discrepancy between experimental and theoretical results in polarized asymmetry, which suggests further improvement, such as including the coupled-channel effect. The predictions for the differential cross section at energy $1.75 < E_\gamma < 5.50$ GeV are presented; these can be checked by future experimental data in the CLAS $eg3$ and $g11$ runs.

ACKNOWLEDGMENTS

This project is partly supported by the National Natural Science Foundation of China under Grants No. 10905077 and No. 11035006.

APPENDIX A: PROPAGATOR

In this Appendix, we will present the propagator of the half-integral-spin particle used in the current work, which is in the same theoretical framework of the Lagrangians in Eqs. (18) and (21) [24–26]. The explicit form of the propagator is

$$G_R^{n+\frac{1}{2}} = \frac{P^{n+\frac{1}{2}}_{\mu_1\mu_2\cdots\mu_n\nu_1\nu_2\cdots\nu_n}}{p^2 - m_R^2 + i m_R \Gamma_R}, \tag{A1}$$

$$P^{n+\frac{1}{2}}_{\mu_1\mu_2\cdots\mu_n\nu_1\nu_2\cdots\nu_n} = \frac{n+1}{2n+3}(\not{p}+m)\gamma^\alpha\gamma^\beta P^{n+1}_{\alpha\mu_1\mu_2\cdots\mu_n\beta\nu_1\nu_2\cdots\nu_n}, \tag{A2}$$

where

$$
\begin{aligned}
&P^{n}_{\mu_1\mu_2\cdots\mu_n\nu_1\nu_2\cdots\nu_n} \\
&= \left(\frac{1}{n!}\right)^2 \sum_{P_{[\mu]}P_{[\nu]}} \Bigg[\prod_{i=1}^{n} \tilde{g}_{\mu_i\nu_i} + a_1 \tilde{g}_{\mu_1\mu_2}\tilde{g}_{\nu_1\nu_2} \prod_{i=3}^{n} \tilde{g}_{\mu_i\nu_i} \\
&\quad + \cdots \\
&\quad + a_r \tilde{g}_{\mu_1\mu_2}\tilde{g}_{\nu_1\nu_2}\tilde{g}_{\mu_3\mu_4}\tilde{g}_{\nu_3\nu_4}\cdots\tilde{g}_{\mu_{2r-1}\mu_{2r}}\tilde{g}_{\nu_{2r-1}\nu_{2r}} \prod_{i=2r+1}^{n} \tilde{g}_{\mu_i\nu_i} \\
&\quad + \cdots \\
&\quad + \begin{cases} a_{n/2}\tilde{g}_{\mu_1\mu_2}\tilde{g}_{\nu_1\nu_2}\cdots\tilde{g}_{\mu_{n-1}\mu_n}\tilde{g}_{\nu_{n-1}\nu_n} & \text{(for even } n\text{)} \\ a_{(n-1)/2}\tilde{g}_{\mu_1\mu_2}\tilde{g}_{\nu_1\nu_2}\cdots\tilde{g}_{\mu_{n-2}\mu_{n-1}}\tilde{g}_{\nu_{n-2}\nu_{n-1}}\tilde{g}_{\mu_n\nu_n} & \text{(for odd } n\text{)} \end{cases} \Bigg] \qquad \text{(A3)} \\
&= \left(\frac{1}{n!}\right)^2 \sum_{P_{[\mu]}P_{[\nu]}} \sum_{r=0}^{[n/2]} a_r \prod_{i=1}^{r} \tilde{g}_{\mu_{2i-1}\mu_{2i}}\tilde{g}_{\nu_{2i-1}\nu_{2i}} \prod_{j=2r+1}^{n} \tilde{g}_{\mu_j\nu_j}, \qquad \text{(A4)}
\end{aligned}
$$

with

$$
a_{r(n)} = \frac{\left(-\frac{1}{2}\right)^r n!}{r!(n-2r)!(2n-1)(2n-3)\cdots(2n-2r+1)}, \qquad \text{(A5)}
$$

where $\tilde{g}_{\mu\nu} = g_{\mu\nu} - \frac{q_\mu q_\nu}{q^2}$, $P_{[\mu]}$ or $P_{[\nu]}$ means the permutations for μ or ν, and $[n]$ means the integer round of n.

Some examples are presented in the following:

$$
G_R^{\frac{1}{2}} = \frac{(\not{p} + m)}{p^2 - m_R^2 + i m_R \Gamma_R}, \qquad \text{(A6)}
$$

$$
G_R^{\frac{3}{2}} = G_R^{\frac{1}{2}} \left(-\tilde{g}_{\mu\nu} + \frac{1}{3}\tilde{\gamma}_\mu\tilde{\gamma}_\nu\right), \qquad \text{(A7)}
$$

$$
G_R^{\frac{5}{2}} = G_R^{\frac{1}{2}} \sum_{P_{[\mu]},P_{[\nu]}}^{2} \left[\frac{1}{4}\tilde{g}_{\mu\nu}\tilde{g}_{\mu\nu} - \frac{1}{20}\tilde{g}_{\mu\mu}\tilde{g}_{\nu\nu} - \frac{1}{10}\tilde{\gamma}_\mu\tilde{\gamma}_\nu\tilde{g}_{\mu\nu}\right], \qquad \text{(A8)}
$$

where $\tilde{\gamma}_\nu = \gamma_\nu - \frac{p_\nu \not{p}}{p^2}$.

APPENDIX B: EXTRACTING THE COUPLING CONSTANTS

As mentioned in Sec. II B, the Lagrangians in Eqs. (18) and (21) show both radiative and strong decay of the nucleon resonance with $J > 1/2$ as described by two coupling constants. In this Appendix we will show how to extract these coupling constants from the helicity amplitudes and partial decay amplitudes.

The helicity amplitudes for the resonances with spin-parity J^P can be calculated from the definition in Eq. (22) easily in the c.m. frame as

$$
A_{\frac{1}{2}}\left(\frac{1}{2}^P\right) = \mathcal{P}\frac{e f_1}{2M_N}\sqrt{\frac{k_\gamma M_R}{M_N}}, \qquad \text{(B1)}
$$

$$
A_{\frac{3}{2}}(J^P) = \mathcal{P}F_{\frac{3}{2}}k_\gamma^{n-1}\frac{e}{\sqrt{2}(2M_N)^n}\sqrt{\frac{k_\gamma M_R}{M_N}}\left[f_1 + \left(\frac{\mathcal{P}}{M_R}\right)\frac{f_2}{4M_N}M_R(M_R + \mathcal{P}M_N)\right], \qquad \text{(B2)}
$$

$$
A_{\frac{1}{2}}(J^P) = \mathcal{P}F_{\frac{1}{2}}k_\gamma^{n-1}\frac{e}{\sqrt{6}(2M_N)^n}\sqrt{\frac{k_\gamma M_N}{M_R}}\left[f_1 + \frac{f_2}{4M_N^2}M_R(M_R + \mathcal{P}M_N)\right], \qquad \text{(B3)}
$$

where $F_r = \prod_{i=2}^{n}\langle 10, i - \frac{1}{2}r | i + \frac{1}{2}r\rangle$ and $\mathcal{P} = P(-1)^n$ with $n = J - \frac{1}{2}$. Here M_N and M_R are the masses of nucleon and the nucleon resonance, and k_γ is the energy of the photon. The helicity amplitudes A_λ can be obtained by CQM or extracted from the experiment. Now the coupling constants for the resonances with $J = \frac{1}{2}$ can be obtained from $A_{1/2}$ directly and the ones with $J > \frac{1}{2}$ can be obtained by solving the two equations for $A_{1/2}$ and $A_{3/2}$.

For the nucleon resonances decay to K and $\Lambda^*(1520)$, we have

$$
\begin{aligned}
\mathcal{A}(J^P, r, \theta) &= \langle K(\boldsymbol{q})\,\Lambda^*(-\boldsymbol{q}, r)| - i\,\mathcal{H}_{\text{int}}|R(\boldsymbol{0}, r)\rangle \\
&= 4\pi M_R\sqrt{\frac{2}{q}}\sum_{\ell}\left\langle \ell\, 0\, \frac{3}{2}\, r \middle| J\, r\right\rangle Y_{\ell 0}G(\ell), \qquad \text{(B4)}
\end{aligned}
$$

if we choose $m_\ell = 0$. Here θ is the angle of the final K. The relative orbital angular momentum ℓ of the final state is constrained by the spin-parity of the resonance. For the nucleon resonances with $J > 1/2$, there are two ℓ, denoted as ℓ_1 and ℓ_2 hereafter.

Since the partial wave decay amplitudes $G(\ell)$ are independent of θ, we choose $\theta = 0$ and reach

$$
A(J^P, \theta = 0, r) = \sqrt{\frac{2\ell_1 + 1}{4\pi}}\left\langle \ell_1\, 0\, \frac{3}{2}\, r \middle| J\, r\right\rangle G(\ell_1) + \sqrt{\frac{2\ell_2 + 1}{4\pi}}\left\langle \ell_2\, 0\, \frac{3}{2}\, r \middle| J\, r\right\rangle G(\ell_2). \qquad \text{(B5)}
$$

The $G(\ell)$ can be obtained from the CQM and is independent on r, so the difference of the amplitudes with different r is from the Clebsch-Gordan coefficient.

With certain $J > \frac{1}{2}$ and r, the decay amplitudes can be calculated and have the form

$$A(J^P, r, \theta = 0) = -\frac{\sqrt{8\pi M_R}}{M_{\Lambda^*}} \frac{q^{n-1}}{m_K^n} \left[h_1 \mathcal{P}[c_{l_0\mathcal{P}} p^0 + (c_{1\mathcal{P}} - c_{l_0\mathcal{P}}) M_{\Lambda^*}] \sqrt{p^0 + \mathcal{P} M_{\Lambda^*}} (M_R - \mathcal{P} M_{\Lambda^*}) + \frac{h_2}{m_K} M_R q^2 c_{l_0\mathcal{P}} \sqrt{p^0 + \mathcal{P} M_{\Lambda^*}} \right], \tag{B6}$$

where $c_{1\pm,l_0\pm} = \prod_{i=2}^{n} \langle 10i - \frac{1}{2} r | i + \frac{1}{2} r \rangle [1, \delta_{l_0 0}] (|\langle 1 l_0 \frac{1}{2} \frac{1}{2} | \frac{3}{2} r \rangle|^2 \pm |\langle 1 l_0 \frac{1}{2} - \frac{1}{2} | \frac{3}{2} r \rangle|^2)$ and $\mathcal{P} = P(-1)^{n+1}$. Here M_{Λ^*} and m_K are masses of the $\lambda(1520)$ and the K meson, and p^0 is the energy of the final $\Lambda(1520)$. Now the coupling constants h_1 and h_2 are related to the partial wave decay amplitudes $G(\ell)$. The h_1 and h_2 can be found from the above equations by choosing $r = 1/2$ and $r = 3/2$.

[1] K. Nakamura *et al*. (Particle Data Group), J. Phys. G **37**, 075021 (2010) and 2011 partial update for the 2012 edition.
[2] S.-H. Kim, S.-I. Nam, Y. Oh, and H.-C. Kim, Phys. Rev. D **84**, 114023 (2011).
[3] A. Kiswandhi and S. N. Yang, Phys. Rev. C **86**, 015203 (2012).
[4] J. F. Zhang, N. C. Mukhopadhyay, and M. Benmerrouche, Phys. Rev. C **52**, 1134 (1995).
[5] K. Nakayama and H. Haberzettl, Phys. Rev. C **73**, 045211 (2006).
[6] X.-H. Zhong and Q. Zhao, Phys. Rev. C **84**, 065204 (2011).
[7] J. He and B. Saghai, Phys. Rev. C **80**, 015207 (2009).
[8] A. Boyarski, R. E. Diebold, S. D. Ecklund, G. E. Fischer, Y. Murata, B. Richter, and M. Sands, Phys. Lett. B **34**, 547 (1971).
[9] D. P. Barber *et al*., Z. Phys. C **7**, 17 (1980).
[10] T. Nakano *et al*. (LEPS Collaboration), Phys. Rev. Lett. **91**, 012002 (2003).
[11] N. Muramatsu *et al*., Phys. Rev. Lett. **103**, 012001 (2009).
[12] S. I. Nam and C. W. Kao, Phys. Rev. C **81**, 055206 (2010).
[13] H. Kohri *et al*. (LEPS Collaboration), Phys. Rev. Lett. **104**, 172001 (2010).
[14] J. J. Xie and J. Nieves, Phys. Rev. C **82**, 045205 (2010).
[15] S. Capstick and W. Roberts, Phys. Rev. D **58**, 074011 (1998).
[16] S. Capstick, Phys. Rev. D **46**, 2864 (1992).
[17] Y. Oh, C. M. Ko, and K. Nakayama, Phys. Rev. C **77**, 045204 (2008).
[18] S. I. Nam, A. Hosaka, and H. C. Kim, Phys. Rev. D **71**, 114012 (2005).
[19] H. Toki, C. Garcia-Recio, and J. Nieves, Phys. Rev. D **77**, 034001 (2008).
[20] T. Hyodo, S. Sarkar, A. Hosaka, and E. Oset, Phys. Rev. C **73**, 035209 (2006); **75**, 029901(E) (2007).
[21] A. I. Titov, B. Kampfer, S. Date, and Y. Ohashi, Phys. Rev. C **72**, 035206 (2005); **72**, 049901(E) (2005).
[22] M. Guidal, J. M. Laget, and M. Vanderhaeghen, Nucl. Phys. A **627**, 645 (1997).
[23] T. Corthals, T. Van Cauteren, J. Ryckebusch, and D. G. Ireland, Phys. Rev. C **75**, 045204 (2007).
[24] S.-J. Chang, Phys. Rev. **161**, 1308 (1967).
[25] J. G. Rushbrooke, Phys. Rev. **143**, 1345 (1966).
[26] R. E. Behrends and C. Fronsdal, Phys. Rev. **106**, 345 (1957).
[27] J. J. Wu, Z. Ouyang, and B. S. Zou, Phys. Rev. C **80**, 045211 (2009).
[28] Z. Zhao, presented at the 8th Workshop on the Physics of Excited Nucleons (NSTAR2011), Newport News, VA, USA, May 2011.
[29] F. W. Wieland *et al*., arXiv:1011.0822 [nucl-ex].